Theoretical Study of Unsymmetrical Bisfullerene and Its Derivatives: C_{131}, $C_{129}BN$, and $C_{130}Si$

Yiying Zheng, Jingping Zhang,* and Godefroid Gahungu

Faculty of Chemistry, Northeast Normal University, Changchun, 130024, China

Received: December 4, 2005; In Final Form: May 1, 2006

Unsymmetrical bisfullerene C_{131} and its derivatives such as $C_{129}BN$ and $C_{130}Si$ are systematically investigated by semiempirical and density functional theory approaches. In comparison with the experimental data, calculated IR and NMR results reveal that both $C_{131}(H)$ and $C_{131}(P)$ isomers are possible compounds to coexist in the synthesized product. The C/Si and CC/BN substitution can change the electronic properties and reactivities compared with the pristine $C_{131}(H)$ and $C_{131}(P)$, respectively.

1. Introduction

The discovery of fullerenes by Kroto and co-workers initiated a new era in carbon chemistry.[1] Fullerene dimers, like the ball-and-chain dimmers,[2] bisfullerenes have attracted attention as models for fullerene polymers, as intermediates for the formation of endohedral fullerenes,[3] or as molecules with interesting properties, such as electronic interactions between the two cages.[4−6] Drageo et al. synthesized the first molecule C_{121}, which is also the only one that has been successfully synthesized to date for the bisfullerene family.[7,8] A theoretical study was reported on C_{121} by the same group.[9] It was revealed that [6,6]-[6,5] (C_s) C_{121} (it has both a methanofullerene and a homofullerene moiety) was the most stable structure among three possible isomers, which was supported by the calculations of energies, IR and Raman spectra, as well as NMR spectra. Recently, Zhao et al. succeeded in synthesis of other two bisfullerenes (C_{141} and C_{131}) using an energetic radiation-catalyzed sandwich reaction.[10,11] Theoretically, they pointed out that the C_{141} had a new structure: two C_{70} side cage open [6,6] ring junctions located at the equator area to create new chemical bonds for the bridge atom.[12]

Recently, Zhao et al. reported that C_{131} has two considerable stable structures: [6,6]-[e,e] (the bridge atom connects the [6,6] bond of C_{60} and the [e,e] bond of C_{70}) and [5,6]-[e,e] (the C_{60} opens the [5,6] bond bridging with the [e,e] bond of C_{70}), the former was predicted to be more stable.[13] However, which of them exist in the synthesized product is still unknown now. With the aim to answer a previous question, both IR and NMR spectra are calculated herein for C_{131} isomers with lower energies and compared to available experimental data.

As it is well-known and exploited in many technological applications, doping is a very efficient way of modifying and tailoring the molecular electronic, superconducting, and nonlinear optical and many other properties of fullerenes.[14−20] To investigate the properties of heterofullerenes derived from C_{131}, such as $C_{130}Si$ and $C_{129}BN$, a set of properties are calculated and compared as well.

2. Computational Methodology

The calculations discussed in this work are all carried out using the Gaussian 98 (revision A.9) program.[21] Geometry pre-optimizations for all possible isomers of C_{131} are performed at AM1[22] and PM3[23] levels. Then two lowest-energy isomers are chosen for high-level (B3LYP[24] with 3-21G,[25,26] 6-31G,[27,28] and 6-31G*[27,28,29] basis sets) re-optimizations. Their vibrational frequencies are predicted at the HF/STO-3G level with the scaling factor (0.8287) and rms (83 cm^{-1}) used by Shimotani et al.[9] ^{13}C NMR shielding values are evaluated with the HF/3-21G method employing the gauge-independent atomic orbital (GIAO)[30] method. The geometries of all the C_{131} derivatives ($C_{130}Si$ and $C_{129}BN$) are calculated at the AM1 level. The selected four lowest-energy isomers of $C_{130}Si$ and six lowest-energy ones of $C_{129}BN$ are re-optimized at high-level DFT approaches (B3LYP/6-31G* for $C_{130}Si$ isomers and B3LYP/6-31G*//B3LYP/3-21G for $C_{129}BN$ ones). The energies of neutral and ionic forms (cation and anion) for $C_{131}(H)$, $C_{131}(P)$, and $C_{131}Si$ isomers, respectively, are calculated at the B3LYP/6-31G* level, and their electron populations are obtained using natural population analysis (NPA).[31]

3. Results and Discussion

3.1. The Stable Structures for C_{131}. 3.1.1. Molecular Geometries of C_{131}. Figure 1 shows (a) two different bond types for C_{60} and (b) eight different bond types for C_{70}. In the case of the [5,6] structure (pentagon−hexagon ring fusion) of C_{60}, the larger moiety of C_{70} faces up to the five- or six-membered ring, leading to the so-called [5,6]/5 or [5,6]/6 isomers (i.e., the optical isomers). As a result, there are 20 possible structural isomers of C_{131}, depending on the bridged position and orientation facial, named from $C_{131}(A)$ to $C_{131}(P)$, whose structures and symmetries are listed in Table 1 (see Supporting Information Figure S1 for description in details).

3.1.2. Relative Stability of C_{131} Isomers and Comparison of the Optimization Methods. The experimental X-ray data for C_{131} is not available yet. Meanwhile, the structure parameters of C_{60}[32] and C_{70}[33,34] were measured by many methods. To compare the efficiency of various calculation methods used for the optimization of fullerene molecules, semiempirical, HF- and B3LYP-optimized structures for both C_{60} and C_{70} are listed in Table S1 (see Supporting Information) compared with available experimental measurements. On the basis of these results, one may find that the HF method with used basis sets and MNDO method fails to accurately describe the molecular geometry for both C_{60} and C_{70}. However, B3LYP-optimized geometries using

* To whom correspondence should be addressed. Fax: +86-431-5684937. E-mail: zhangjp162@nenu.edu.cn.

10.1021/jp0570519 CCC: $33.50
Published on Web 07/26/2006

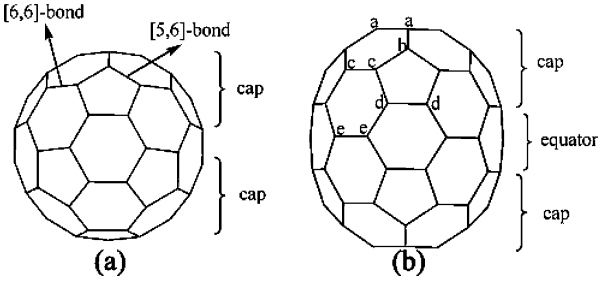

Figure 1. Structures and labeled C−C bond types for (a) C_{60} (I_h) and (b) C_{70} (D_{5h}).

TABLE 1: Names, Structures, Symmetries, and Relative Energies (E_R in kcal/mol) for 20 Possible Isomers of C_{131}

name	structure	symmetry	E_R1[a]	E_R2[b]
C131(A)	[a,a]-[5,6]	C_1	0	0
C131(Ba)	[a,b]-[5,6]/5	C_s	2.975	−3.564
C131(Bb)	[a,b]-[5,6]/6	C_s	2.975	−3.558
C131(Ca)	[b,c]-[5,6]/5	C_1	2.836	2.960
C131(Cb)	[b,c]-[5,6]/6	C_1	2.836	2.959
C131(D)	[c,c]-[5,6]	C_1	3.275	−3.859
C131(Ea)	[c,d]-[5,6]/5	C_1	9.708	8.944
C131(Eb)	[c,d]-[5,6]/6	C_1	9.824	9.046
C131(F)	[d,d]-[5,6]	C_1	10.792	5.570
C131(Ga)	[d,e]-[5,6]/5	C_1	18.979	11.167
C131(Gb)	[d,e]-[5,6]/6	C_1	19.071	11.243
C131(H)	[e,e]-[5,6]	C_s	−6.342	−7.819
C131(I)	[a,a]-[6,6]	C_s	2.029	−4.725
C131(J)	[a,b]-[6,6]	C_s	9.639	−3.188
C131(K)	[b,c]-[6,6]	C_1	4.981	−1.650
C131(L)	[c,c]-[6,6]	C_s	10.077	−3.420
C131(M)	[c,d]-[6,6]	C_1	11.645	4.053
C131(N)	[d,d]-[6,6]	C_s	16.534	5.053
C131(O)	[d,e]-[6,6]	C_1	25.366	11.131
C131(P)	[e,e]-[6,6]	C_{2v}	−5.673	−13.950

[a] Relative energy calculated at AM1 with respect to the C_{131}(A) isomer. [b] Relative energy calculated at PM3 level with respect to the C_{131}(A) isomer.

the basis sets 6-31G, 6-31G* show a good agreement with the experimental data. Indeed, within B3LYP results, no more than 0.013 Å of deviation is observed when 6-31G* basis set is used for C_{60}, and 0.014 Å is the greatest deviation predicted by 6-31G for C_{70}. Meanwhile, the semiempirical (AM1 and PM3) parameters are found to deviate the experimental values by no more than 0.021 Å.

In consideration of both the large size of C_{131} and the accuracy of method, these 20 isomers are pre-optimized by two semiempirical levels: (a) AM1 and (b) PM3, respectively. In Table 1, we list the relative energies with respect to the C_{131}(A) isomer (see detail in Supporting Information Figure S2). It is shown in Table 1 that two isomers (C_{131}(H) and C_{131}(P)) possess lower energy compared with the rest of the isomers. Hence these two isomers are chosen and re-optimized at the B3LYP/3-21G, B3LYP/6-31G, and B3LYP/6-31G* levels, respectively. It is found that the energy of C_{131}(P) is only ∼6.55 kcal/mol lower than that of C_{131}(H) at B3LYP/6-31G* level. These results are compared well with those calculated by Zhao et al.[12] In addition, the same energy difference is also observed with 3-21G and 6-31G basis sets.

The selected parameters of C_{131}(H) and C_{131}(P) with different approaches are listed in Table S2 (Supporting Information); the labeling scheme for the central bridge part is shown in Figure 2. B3LYP method with the 3-21G, 6-31G, and 6-31G* basis sets can obtain almost the same geometries and relative energies. Thus, to save computational time, we can use either the 3-21G or 6-31G basis sets to optimize the structure by the density

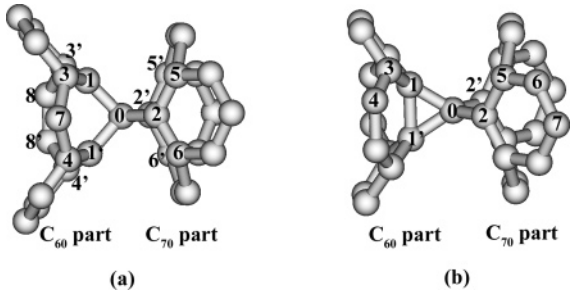

Figure 2. Numbering systems of the carbon atoms in the bridging moiety of (a) C_{131}(H) and (b) C_{131}(P).

functional theory (DFT) approach, then calculate the single-point energy for optimized system at DFT/6-31G* level with higher accuracy. It is worth noting that the AM1-optimized geometry is found to be quite similar to those obtained at DFT higher levels. Therefore, AM1 is a practical method for primary optimization for this kind of compound, although it deviates slightly in energy calculation. However, there is a dramatic deviation for the PM3 predicted parameters for C_{131}(H) compared with other models. Taking the central bridging site as an example, the C1−C1′ distance and C1−C0−C1′ bond angle are found to deviate from other values by ∼0.6 Å and ∼28.5°, respectively. The obvious deviation leads to a closed structure of C_{60} monomer at PM3 level rather than the opened structure predicted by other methods.

3.1.3. Calculated ^{13}C NMR Chemical Shifts for C_{131}(H) and C_{131}(P). Molecules can be identified by their characteristic spectra; the ^{13}C NMR chemical shifts which are known as a powerful technique for determining bisfullerene structures are calculated in this work, for the purpose of confirming the existence of C_{131}(H) and/or C_{131}(P) in experimental work.[10] The NMR results for C_{131}(H) and C_{131}(P) are obtained by applying the GIAO-HF/3-21G method on the B3LYP/6-31G*-optimized structure. For C_{131}(H), the calculated chemical shifts for sp^2 carbons are in the range from 112.36 to 144.44 ppm, which match the experimental measurement well (from 117 to 140 ppm[10]). Furthermore, the obtained chemical shift at 52.06 ppm in the sp^3 region, which is assigned to the intermediate bridge carbon atom, is in good agreement with the experimental data (59.78 ppm). While for C_{131}(P), the obtained chemical shifts for carbons in the sp^2 region are in the range from 119.46 to 143.04 ppm, matching the experimental values well. In the sp^3 region, the calculated chemical shifts are 38.97 ppm for the central bridge atom and two degenerate ones (63.43 ppm) for the bridgehead carbons of C_{60} monomer. The later chemical shifts agree with the experiment well, in the range from 61.57 to 64.49 ppm. The former one, however, is ∼20 ppm smaller than the experimental data. This may result from the basis set effect of NMR calculation.[35] Therefore, one can conclude that both C_{131}(H) and C_{131}(P) are the most possible isomers existing in the synthesized mixture.

3.1.4. IR-Active Vibrational Modes and Intensities for C_{131}(H) and C_{131}(P). With the aim to investigate C_{131} structure further, the IR-active vibrational modes and intensities for C_{131}-(H) and C_{131}(P) are calculated at the HF/STO-3G//B3LYP/6-31G* level as used in the calculation of C_{121}.[9] From the FT-IR spectra measurements,[10] beside the presence of C_{60} and C_{70} that was verified, a peak of bridged part skeletal (1025.8 cm^{-1}) was also observed, confirming the existence of the intermediate bridge part of the two monomers. The computed results are presented in Table 2, where experimental data are listed as well.

In general, the calculated results for both compounds agree with the experimental data. Especially the calculated vibrational

TABLE 2: Selected IR-Active Vibrational Wavenumbers (cm^{-1}) and IR Scattering Actives ($Å^4$/amu) for $C_{131}(H)$ and $C_{131}(P)$ at HF/STO-3G//B3LYP6-31G* Level (after scaled)

$C_{131}(H)$		$C_{131}(P)$		
frequency	IR active	frequency	IR active	exp[a]
1464.9	5.3	1459.7	35.3	1463
1429.4	36.7	1430.4	40.9	1430
1358.9	22.8	1358.9	22.9	1360
1274.8	24.7	1260.8	40.6	1270
1187.2	3.7	1198.6	12.9	1182
1148.5	19.0	1127.7	4.4	1130
1082.4	6.9	1069.4	2.8	1072
1015.8	22.8	1017.8	4.7	1025.8

[a] Data from ref 10.

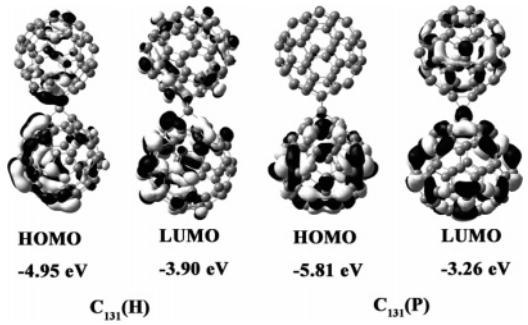

Figure 3. Molecular orbital amplitude plots and energies of the FMOs of $C_{131}(H)$ and $C_{131}(P)$ calculated at B3LYP/6-31G* level.

wavenumbers for the bridged part skeletal stretch are 1015.8 and 1017.8 cm^{-1} for $C_{131}(H)$ and $C_{131}(P)$, respectively, that match the experimental data (1025.8 cm^{-1}) well. However, the intensity of IR activity for $C_{131}(P)$ (4.7) is much weaker than that for $C_{131}(H)$ (22.8). It can be traced back to the higher symmetry of $C_{131}(P)$ (C_{2v}) compared with that of $C_{131}(H)$ (C_s). Consequently, our calculated IR results suggest that both $C_{131}(H)$ and $C_{131}(P)$ may exist in the synthesized mixture.

3.1.5. Frontier Molecular Orbitals Analysis. Figure 3 shows the frontier molecular orbitals (FMO) for $C_{131}(H)$ and $C_{131}(P)$ at B3LYP/6-31G* level. Similar FMO surfaces distribution pattern is found for these two isomers: the highest-occupied molecular orbitals (HOMOs) are mainly localized on the C_{70} monomer, while the lowest-unoccupied molecular orbitals (LUMOs) are distributed on the whole molecule. However, the distribution regions for FMOs are different between them. For the HOMO of $C_{131}(P)$, it is almost uniformly delocalized on C_{70} monomer, whereas the HOMO of $C_{131}(H)$ is mainly localized on the moiety faced up to the C_{60}'s six-member ring of the C_{70} monomer, and a slight contribution is also observed in the C_{60} part. The same tendency is also observed in the distribution of LUMOs. This can be traced back to their different symmetries.

According to Koopmans' theorem, IP $= -E_H$ (E_H = the HOMO energy), and EA $= -E_L$ (E_L = the LUMO energy). IP and EA represent ionization potential and electron affinity, respectively. E_H is found to be -4.95 eV for $C_{131}(H)$, 0.86 eV higher than that for $C_{131}(P)$. While E_L is calculated at -3.90 eV for $C_{131}(H)$, 0.64 eV lower than that for $C_{131}(P)$. This indicates that $C_{131}(H)$ may more easily lose or receive electrons than $C_{131}(P)$. In addition, the HOMO$-$LUMO energy gap (E_G) for $C_{131}(P)$ (2.55 eV) is significantly larger than that for $C_{131}(H)$ (1.05 eV), suggesting that $C_{131}(P)$ is a more stable isomer compared with $C_{131}(H)$ in the ground state.

3.2. The Stability and Properties of $C_{130}Si$. 3.2.1. Electronic Structure. Silicon is a very interesting element for doping fullerenes.[18] Indeed, SiC compounds exhibit desirable properties such as polymorphism, variable band gaps, extraordinary hardness, etc. Considering the successful synthesis of many Si-doped fullernes,[20] it is reasonable to expect that silicon doped bisfullerenes would be synthesized and detected experimentally if appropriate synthetic protocols are achieved.

TABLE 3: Substitution Sites, Relative Energies (E_R, kcal/mol), HOMO Energies (E_H, eV), LUMO Energies (E_L, eV) and HOMO$-$LUMO Gap Energies (E_G, eV) for Four $C_{130}Si$ Isomers

species	substitution sites[a]	E_R[b]	E_H	E_L	E_G
C130Si(HA)	Si0	0.00	-5.74	-3.27	2.46
C130Si(HB)	Si1	-5.77	-5.59	-3.46	2.13
C130Si(PA)	Si0	-12.34	-5.58	-3.36	2.22
C130Si(PB)	Si1	-14.63	-5.73	-3.37	2.36

[a] See Figure 2 for labeling scheme. [b] E_R is with respect to $C_{130}Si(H_A)$.

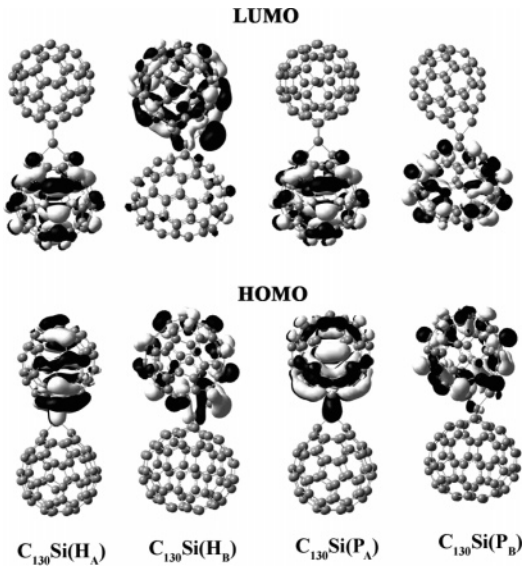

Figure 4. Molecular orbital surfaces (0.02 e au^{-3}) of the HOMO (lower panel) and LUMO (upper panel) for $C_{130}Si(H_A)$, $C_{130}Si(H_B)$, $C_{130}Si(P_A)$, and $C_{130}Si(P_B)$.

For the purpose of investigating the stability and properties of C/Si substituted C_{131}, we substitute the central bridge and bridgehead carbon atoms by silicon in $C_{131}(H)$ and $C_{131}(P)$. The selected four possible C/Si substituted isomers for $C_{131}(H)$ and 3 ones for $C_{131}(P)$ are listed in Table S3 (see Supporting Information). After the optimization with AM1 method, four more stable isomers are chosen for high level calculation. As summarized in the second column of Table 3, both $C_{130}Si(H_A)$ and $C_{130}Si(P_A)$ are the isomers whose central bridge carbons are substituted by Si, respectively, while for both $C_{130}Si(H_B)$ and $C_{130}Si(P_B)$, the C/Si substitution sites are on the bridgehead carbon of C_{60} monomer.

Table 3 summarizes the B3LYP/6-31G*-calculated E_R, E_H, E_L, and E_G of the four selected $C_{130}Si$ isomers. One may find that the energies of C/Si substituted isomers of $C_{131}(P)$ are slightly lower than those of $C_{131}(H)$, with $C_{130}Si(P_B)$, i.e., one of the formers, possessing the lowest energy. Moreover, the C/Si substitution significantly changes the electronic properties compared with those for $C_{131}(H)$ and $C_{131}(P)$. Indeed, the C/Si substitution leads to the decrease of E_H and the increase of E_L in $C_{131}(H)$. As a result, the E_G values for $C_{130}Si(H_A)$ and $C_{130}Si(H_B)$ are much greater than that for $C_{131}(H)$, corresponding to more stable ground states. However, a reverse trend is observed in the C/Si substitution derivatives of $C_{131}(P)$. Correspondingly, the FMOs of $C_{130}Si$ as shown in Figure 4 are different from those of $C_{131}(H)$ and $C_{131}(P)$, where the HOMOs

TABLE 4: S^+, S^-, S^+/S^-, and S^-/S^+ Values of the Relevant Atomic Positions for $C_{131}(H)$, $C_{130}Si(H_A)$, $C_{130}Si(H_B)$, C_{131} (P), $C_{130}Si(P_A)$, and $C_{130}Si(P_B)$

species	atom	S^+	S^-	S^+/S^-	S^-/S^+
C_{131} (H)	C0	0.000	0.000		
	C1	0.001	0.002	0.500	2.000
$C_{130}Si(H_A)$	Si0	0.001	0.002	0.500	2.000
$C_{130}Si(H_B)$	Si1	0.017	0.026	0.654	1.529
C_{131} (P)	C0	0.001	0.003	0.333	3.000
	C1	0.000	0.000		
$C_{130}Si(P_A)$	Si0	0.001	0.008	0.125	8.000
$C_{130}Si(P_B)$	Si1	0.001	0.009	0.111	9.000

are all mainly localized on the C_{60} monomer instead of on C_{70} monomers for $C_{131}(H)$ and $C_{131}(P)$. A significant difference is observed for $C_{130}Si(H_B)$ whose LUMO is mainly localized on C_{60} monomer, while those for the other isomers are mainly localized on the C_{70} monomers.

3.1.2. Reactivity for Silicon in $C_{130}Si$ Isomers. Because of the electronegativity difference between the heteroatom and the carbon atom, it is necessary to investigate the reactivities of interested atoms before and after the substitution. To predict the intramolecular and intermolecular reactivity, the relative electrophilicity (S^+/S^-) and nucleophilicity (S^-/S^+) are calculated as proposed by Roy et al.[36] The atomic softness values (S^+ and S^-) is defined by eqs 1 and 2[37]

$$S^+ = [\rho_A(N+1) - \rho_A(N)]S \quad \text{(suited for studies of nucleophilic attack)} \quad (1)$$

$$S^- = [\rho_A(N) - \rho_A(N-1)]S \quad \text{(suited for studies of electrophilic attack)} \quad (2)$$

$$S = 1/(IP - EA) \quad (3)$$

Here $\rho_A(N)$ represents the electronic population on atom A for the N electron system. The global softness (S) is described in eq 3. For a certain atom, if $S^+/S^- > S^-/S^+$, then it is the preferred electrophilic site and vice versa. For different atoms in same/different molecules, the highest S^+/S^- corresponds to the most probability of being attacked by a nucleophile (Nu^-), and the site having the highest S^-/S^+ is the most probable site to be attacked by an electrophile (El^+).

TABLE 5: Substitution Site, Structures, Relative Energies (E_R), HOMO Energies (E_H), LUMO Energies (E_L), and HOMO−LUMO Energies (E_G) for Six $C_{129}BN$ Isomers

species	substitution site[a]	E_R[b]	E_H	E_L	E_G
$C_{129}BN(H_{Ea})$	B1, N3	0.00	−5.70	−3.30	2.40
$C_{129}BN(H_{Eb})$	B3, N1	2.60	−5.70	−3.30	2.39
$C_{129}BN(H_J)$	B8, N8	−0.07	−5.77	−3.24	2.53
$C_{129}BN(P_{Db})$	B5, N2	3.76	−5.59	−3.28	2.31
$C_{129}BN(P_{Ea})$	B3, N4	−5.47	−5.47	−3.26	2.54
$C_{129}BN(P_{Eb})$	B4, N3	0.44	−5.76	−3.29	2.48

[a] See Figure 2 for labeling scheme. [b] E_R is with respect to $C_{129}BN(H_{Ea})$.

In Table 4, we list the S^+, S^-, S^+/S^-, and S^-/S^+ values for the atoms of interest. It can be found that C/Si substitution results in the changes of reactivity for interested atoms. For $C_{131}(H)$, C0 is a neutral site (both S^+ and S^- values are zero) and C1 is a nucleophilic one ($S^-/S^+ > S^+/S^-$). After the C/Si substitution, Si0 changes to a nucleophilic site with $S^-/S^+ > S^+/S^-$ for $C_{130}Si(H_A)$. While for $C_{130}Si(H_B)$, Si1 is more electrophilic ($S^+/S^- = 0.654$) than the pristine C1 (0.500). However, it is still a preferred nucleophilic site with S^-/S^+ (1.529) > S^+/S^- (0.654). For $C_{131}(P)$, the C0 is a nucleophilic site with $S^-/S^+ > S^+/S^-$, C1 being a neutral one (S^+, $S^- \approx 0.000$). The C substitution by Si in $C_{131}(P)$ results in more nucleophilicity for both Si0 ($S^-/S^+ = 8.000$) in $C_{130}Si(P_A)$ and Si1 ($S^-/S^+ = 9.000$) in $C_{130}Si(P_B)$ than those in $C_{131}(P)$ ($S^-/S^+ = 3.000$). Furthermore, Si1 in $C_{130}Si(P_B)$ is the most nucleophilic one among all investigated sites. These results compare well with those reported by Masenelli et al. in their theoretical study on $Si-(C_{60})_2$ that observed that Si has nucleophilic character.[38]

3.3. The Stability and Properties of $C_{129}BN$. 3.3.1. Electronic Structures. BN is an isoelectronic equivalent of CC. The CC/BN substitution is expected to change the structure and nature of the bisfullerenes. In this work, the carbon atoms around the central bridge atom are substituted by BN unit. Then 18 possible CC/BN substitution isomers for $C_{131}(H)$ and 11 ones for $C_{131}(P)$ are optimized at AM1 level (See Supporting Information Table S4 in detail). Six isomers with lower energies are chosen for high-level studies. Three derivatives are from $C_{131}(H)$ and another three ones from $C_{131}(P)$; their corresponding substitution sites are listed in the second column of Table 5.

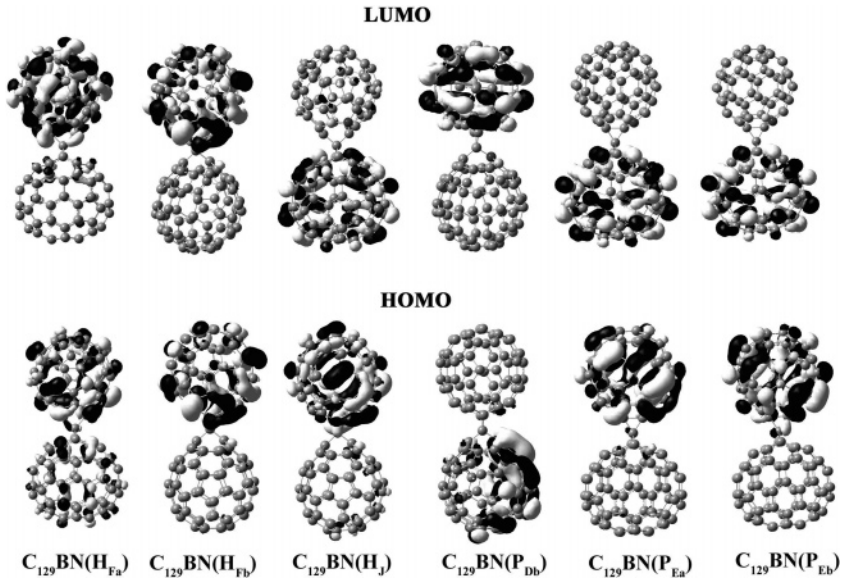

Figure 5. Molecular orbital surfaces (0.02 e au^{-3}) of the HOMO (lower) and LUMO (upper) for $C_{129}BN(H_{Fa})$, $C_{129}BN(H_{Fb})$, $C_{129}BN(H_J)$, $C_{129}BN(P_{Db})$, $C_{129}BN(P_{Ea})$, and $C_{129}BN(P_{Eb})$.

TABLE 6: S^+, S^-, S^+/S^-, and S^-/S^+ Values of the Relevant Atomic Positions for C_{131}(P), $C_{129}BN(P_{Ea})$, C_{131}(H), and $C_{129}BN(H_J)$

species	atom	S^+	S^-	S^+/S^-	S^-/S^+
C_{131}(P)	C3	0.001	0.003	0.333	3.000
	C4	0.001	0.004	0.250	4.000
$C_{129}BN(P_{Ea})$	B3	0.001	0.003	0.333	3.000
	N4	0.001	0.002	0.500	2.000
C_{131}(H)	C8	0.003	0.001	3.000	0.333
	C8′	0.003	0.001	3.000	0.333
$C_{129}BN(H_J)$	B8	0.003	0.005	0.800	1.667
	N8′	0.002	0.003	0.667	1.500

The B3LYP/6-31G*//B3LYP/3-21G-calculated energies of E_R, E_H, E_L, and E_G for the six $C_{129}BN$ isomers are listed in Table 5. From the calculated results, it is found that the energies of these six isomers are very close with each other and $C_{129}BN(P_{Ea})$ possesses the lowest energy. In comparison with C_{131}(H), its $C_{129}BN$ derivatives have lower E_H and higher E_L values. Consequently, their HOMO−LUMO gaps are larger than that of C_{131}(H), indicating that CC/BN substitutions favor for the stabilities of their ground state. While the CC/BN substitution of C_{131}(P) only slightly changes the E_H, E_L, and E_G values for corresponding isomers.

For a better understanding of the influence of the substitution on the electronic structure, we show their FMOs in Figure 5. A significant difference is observed for $C_{129}BN(P_{Db})$, whose HOMO is mainly localized on C_{70} monomer instead of C_{60} monomers for the other derivatives. It can be traced back to the CC/BN substitution sites of $C_{129}BN(P_{Db})$, in which the BN unit substitute the CC on the C_{70} monomer instead of C_{60} monomer (for other derivatives). However, LUMOs are mainly localized on the C_{60} monomers for $C_{129}BN(H_{Fa})$, $C_{129}BN(H_{Fb})$, and $C_{129}BN(P_{Db})$, while they are mainly localized on the C_{70} monomers for the rest three derivatives. These features indicate the significant change of electronic structures after CC/BN substitution.

3.3.2. Reactivity for BN in $C_{129}BN$ Isomers. With the aim to investigate the reactivity of CC/BN substitution sites, the calculated S^+, S^-, S^+/S^-, and S^-/S^+ values for interested atoms in $C_{129}BN(P_{Ea})$ and $C_{129}BN(H_J)$ those possess lower relative energy values, are given in Table 6. For the ease of comparison, corresponding atoms in C_{131}(H) and C_{131}(P) are listed as well.

From the calculated results, it can be found that the change of reactivity is CC/BN substitution sites dependent. For C_{131}(P), both C3 and C4 are nucleophilic sites with $S^-/S^+ > S^+/S^-$. Slight changes are observed for both B3 and N4 in $C_{129}BN(P_{Ea})$ after CC/BN substitution, with the slight increase of S^+/S^-. While for C_{131}(H), both C8 and C8′ are electrophilic sites, whose S^+/S^- (3.000) are larger than S^-/S^+ (0.333). However, S^-/S^+ for both of the substituted B8 and N8′ in $C_{129}BN(H_J)$ is significant increasing, with B8 being more nucleophilic ($S^-/S^+ = 1.667$) than N8′ ($S^-/S^+ = 1.500$). In addition, for both $C_{129}BN(P_{Ea})$ and $C_{129}BN(H_J)$, B is more favored by electrophilic attack than N.

4. Conclusion

In this article, we reported the structures and stabilities of C_{131}, $C_{129}BN$, and $C_{130}Si$. The main conclusions from this study are as following: Among 20 possible structures of C_{131}, C_{131}(H), and C_{131}(P) process lower energies than other isomers. The calculated IR and NMR spectra all suggest that both of them may exist in the synthesized product. Both C/Si and CC/BN substitution can change the electronic properties and reactivities of pristine C_{131}(H) and C_{131}(P). C/Si and CC/BN substitution can alter the distribution for FMOs and energy gaps for the derivatives of C_{131}(H/P). The heteroatom Si in $C_{130}Si$ isomers with lower energies is a nucleophilic site after C/Si substitution, while the changes of reactivity for $C_{129}BN$ isomers with lower energies are CC/BN substitution sites dependent.

Acknowledgment. Financial supports from the National Natural Science Foundation of China (No. 50473032), SRF for ROCS, SEM, and Outstanding Youth Project of Jilin Province are gratefully acknowledged.

Supporting Information Available: Computed bond lengths (Å) of C_{60} (I_h) and C_{70} (D_{5h}) at different levels, selected structural parameters for C_{131}(H) (C_s) and C_{131}(P) (C_{2v}) with different methods. names, structures, and relative energies (E_R) for $C_{130}Si$ and $C_{129}BN$ isomers at the AM1 level, structures of 20 possible isomers of C_{131}, and dependence of relative energies of 20 C_{131} isomers at the (a) AM1 and (b) PM3 levels. This material is available free of charge via the Internet at http://pubs.acs.org.

References and Notes

(1) Kroto, H. W.; Heath, J. R.; O'Brien, S. C.; Curl, R. F.; Smalley, R. E. *Nature* **1985**, *318*, 162.
(2) Shvartsburg, A. A.; Hudgins, R. R.; Gutierrez, R.; Jungnickel, G.; Frauenheim, T.; Jackson, K. A.; Jarrold, M. F. *J. Phys. Chem. A* **1999**, *103*, 5275.
(3) Patchkovskii, S.; Thiel, W. *J. Am. Chem. Soc.* **1998**, *120*, 556.
(4) Hummelen, J. C.; Knight, B.; Pavlovich, J.; Gonzales, R.; Wudl, F. *Science* **1995**, *269*, 1554.
(5) Balch, A. L.; Costa, D. A.; Fawcett, W. R.; Winkler, K. *J. Phys. Chem.* **1996**, *100*, 4823.
(6) Dragoe, N.; Shimotani, H.; Hayashi, M.; Saigo, K.; de Bettencourt-Dias, A.; Balch; A. L.; Miyake, Y.; Achiba; Y.; Kitazawa, K. *J. Org. Chem.* **2000**, *65*, 3269.
(7) Dragoe, N.; Shimotani, H.; Wang, J.; Iwaya, M.; de Bettencourt-Dias, A.; Balch, A. L.; Kitazawa, K. *J. Am. Chem. Soc.* **2001**, *123*, 1294.
(8) Dragoe, N.; Tanibayashi, S.; Nakahara, K.; Nakao, S.; Shimotani, H.; Xiao, L.; Kitazawa, K.; Kitazawa, K.; Achiba, Y.; Kikuchi, K.; Nojima, K. *Chem. Commun.* **1999**, 85.
(9) Shimotani, H.; Dragoe, N.; Kitazawa, K. *J. Phys. Chem. A* **2001**, *105*, 4980.
(10) Zhao; Y.; Chen, Z.; Yuan, H.; Gao; X.; Qu, L.; Chai, Z.; Xing, G.; Yoshimoto, S.; Tsutsumi, E.; Itaya, K. *J. Am. Chem. Soc.* **2004**, *126*, 11134.
(11) Chen, Z.; Zhao, Y.; Qu, L.; Gao, X.; Zhang, J.; Yuan, H.; Chai, Z.; xing, G.; Cheng, Y. *Chin. Sci. Bull.* **2004**, *49*, 225.
(12) Gao, X.; Yuan, H.; Chen, Z.; Zhao, Y. *J. Comput. Chem.* **2004**, *25*, 2023.
(13) Gao, X.; Zhao, Y.; Yuan, H.; Chen, Z.; Chai, Z. *Chem. Phys. Lett.* **2006**, *418*, 24.
(14) Chen, Z.; Ma, K.; zhao, H.; Pan, Y.; Zhao, X.; Tang, A.; Feng, J. *THEOCHEM* **1999**, *466*, 127.
(15) Chen, Z.; Ma, K.; Pan, Y.; Zhao, X.; Tang, A. *THEOCHEM* **1999**, *490*, 61.
(16) Pattanayak, J.; Kar, T.; Scheiner, S. *J. Phys. Chem. A* **2004**, *108*, 7681.
(17) Piechota, J.; Byszewski, P.; Jablonski, R.; Antonova, K. *Fullerene Sci. Technol.* **1996**, *4*, 491.
(18) Marcos, P. A.; Alonso, J. A.; Molina, L. M.; Rubio, A.; López, M. J. *J. Chem. Phys.* **2003**, *119*, 1127.
(19) Chen, Z.; Ma, K.; Shang, Z.; Pan, Y.; Zhao, X.; Tang, A. *Acta Chim. Sin.* **1999**, *57*, 712.
(20) Pellarin, M.; Ray, C.; Lermé, J.; Vialle, J. L.; Broyer, M.; Mélinon, P. *J. Chem. Phys.* **2000**, *112*, 8436.
(21) Frisch, M. J.; Trucks, G. W.; Schlegel, H. B.; Scuseria, G. E.; Robb, M. A.; Cheeseman, J. R.; Zakrzewski, V. G.; Montgomery, J. A., Jr.; Stratmann, R. E.; Burant, J. C.; Dapprich, S.; Millam, J. M.; Daniels, A. D.; Kudin, K. N.; Strain, M. C.; Farkas, O.; Tomasi, J.; Barone, V.; Cossi, M.; Cammi, R.; Mennucci, B.; Pomelli, C.; Adamo, C.; Clifford, S.; Ochterski, J.; Petersson, G. A.; Ayala, P. Y.; Cui, Q.; Morokuma, K.; Malick, D. K.; Rabuck, A. D.; Raghavachari, K.; Foresman, J. B.; Cioslowski, J.; Ortiz, J. V.; Stefanov, B. B.; Liu, G.; Liashenko, A.; Piskorz, P.; Komaromi, I.; Gomperts, R.; Martin, R. L.; Fox, D. J.; Keith, T.; Al-Laham, M. A.; Peng, C. Y.; Nanayakkara, A.; Gonzalez, C.; Challacombe, M.; Gill, P. M. W.; Johnson, B. G.; Chen, W.; Wong, M. W.; Andres, J. L.; Head-Gordon, M.; Replogle, E. S.; Pople, J. A. *Gaussian 98*; Gaussian, Inc.: Pittsburgh, PA, **1998**.

(22) Dewar, M. J. S.; Zoebisch, E. G.; Healy, E. F.; Stewart, J. J. P. *J. Am. Chem. Soc.* **1985**, *107*, 3902.
(23) Stewart, J. J. P. *J. Comput. Chem.* **1989**, *10*, 209.
(24) Stephens, P. J.; Devlin, F. J.; Chabalowski, C. F.; Frisch, M. J. *J. Phys. Chem.* **1994**, *98*, 11623.
(25) Binkly, J. S.; Pople, J. A.; Hehre, W. J. *J. Am. Chem. Soc.* **1980**, *102*, 939.
(26) Gordon, M. S.; Binkley, J. S.; Pople, J. A.; Pietro, W. J.; Hehre, W. J. *J. Am. Chem. Soc.* **1982**, *104*, 2797.
(27) Hariharan, P. C.; Pople, J. A. *Mol. Phys.* **1974**, *27*, 209.
(28) Gordon, M. S. *Chem. Phys. Lett.* **1980**, *76*, 163.
(29) Frisch, M. J.; Pople, J. A.; Binkley J. S. *J. Chem. Phys.* **1984**, *80*, 3265.
(30) Wolinski, K.; Hinton, J. F.; Pulay, P. *J. Am. Chem. Soc.* **1990**, *112*, 8251.
(31) Reed, A. E.; Curtiss, L. A.; Weinhold, F. *Chem. Rev.* **1988**, 88, 899.
(32) Hedberg, K.; Hedberg, L.; Bethune, D. S.; Brown, C. A. Dorn, H. C. Johnson, R. D.; de Vries, M. *Science* **1991**, *254*, 410.
(33) Burgi, H. B.; Venugopalan, P.; Schwarzenbach, D.; Diederich, F.; Thilgen, C. *Helv. Chim. Acta* **1993**, *76*, 2155.
(34) Nikolaev, A. V.; Dennis, T. J. S.; Prassides, K.; Soper, A. K. *Chem. Phys. Lett*. **1994**, *223*, 143.
(35) Cheeseman, J. R.; Trucks, G. W.; Keith, T. A.; Frisch, M. J. *J. Chem. Phys.* **1996**, *104*, 5497.
(36) Roy, R. K.; Krishnamurthy, S.; Geerlings, P.; Pal, S. *J. Phys. Chem. A* **1998**, *102*, 3746.
(37) Yang, W.; Mortier, W. J. *J. Am. Chem. Soc.* **1986**, *108*, 5708.
(38) Masenelli, B.; Tournus, F.; Mélinon, P.; Pérez, A.; Blase, X. *J. Chem. Phys.* **2002**, *117*, 10627.